Journal of Integrative Neuroscience

J. Integr. Neurosci. **2025**; 24(9): 42984
https://doi.org/10.31083/JIN42984

Original Research

HAP1 Promotes Spinal Cord Injury Recovery Through BDNF Signaling Modulation

Xinzhou Xiao[1], Riyun Yang[1], Yongjiang Wu[1], Feifei Long[1], Hongjun Zhao[1], Jingying Pan[1,*]

[1]Department of Histology and Embryology, Medical School of Nantong University, 226001 Nantong, Jiangsu, China
*Correspondence: panjingying0505@126.com (Jingying Pan)
Academic Editor: Nuno A. Silva
Submitted: 5 June 2025 Revised: 31 July 2025 Accepted: 6 August 2025 Published: 25 September 2025

Abstract

Background: Spinal cord injury (SCI) is a severe medical condition resulting from trauma, disease or degeneration, leading to partial or complete loss of sensory and motor functions. Huntingtin-associated protein 1 (HAP1) is a classical neuronal protein that plays a crucial role in the nervous systems. Although numerous proteins and molecules have been extensively studied, the mechanisms underlying SCI pathogenesis remain incompletely understood. This study aimed to elucidate how HAP1 modulates functional recovery and tissue repair post-SCI through a multifaceted experimental approach. **Methods**: Immunofluorescence staining was used to evaluate the spatial distribution and expression levels of HAP1 in spinal cord. An SCI model was established to assess behavioral functions using the Basso Mouse Scale, forced swim, inclined plate and hot plate tests. Luxol fast blue staining was used to assess morphological repair. The protein and mRNA expression levels of brain-derived neurotrophic factor (BDNF) were quantified post-SCI using enzyme-linked immunosorbent assay and quantitative real-time polymerase chain reaction, respectively. To elucidate the functional role of HAP1 in the SCI process, BDNF injections and behavioral tests were performed. Finally, RNA sequencing followed by bioinformatics analyses (Kyoto Encyclopaedia of Genes and Genomes (KEGG) pathways and Gene Ontology (GO) term enrichment) were performed to identify differentially expressed genes and signaling pathways associated with HAP1 in the SCI process. **Results**: HAP1 is abundantly expressed in spinal cord neurons and plays a crucial role in post-traumatic recovery. HAP1 deficiency significantly impairs both functional recovery and morphological repair following spinal cord injury. Comparative analysis revealed lower BDNF levels in HAP1 heterozygous (HET) mice than in wild-type (WT) controls post-injury. Exogenous BDNF administration partially rescued behavioral deficits in HET mice, indicating BDNF-dependent compensatory mechanisms. RNA-seq analysis identified 444 differentially expressed genes and potential pathways associated with HAP1 in the SCI process. **Conclusions**: HAP1 significantly enhances functional recovery and morphological repair post-SCI through potentiation of BDNF signaling pathways. These findings position HAP1 as a novel therapeutic target for SCI treatment.

Keywords: spinal cord injuries; huntingtin-associated protein 1; brain derived neurotrophic factor; behavioral research; pathway analysis

1. Introduction

Spinal cord injury (SCI) is a debilitating neurological condition marked by acute structural damage and progressive secondary pathological cascades, that lead to chronic disability and serious complications. This disorder imposes significant socioeconomic burdens and profoundly impairs a patient's quality of life [1–3]. SCI pathogenesis involves: primary mechanical damage (structural disruption/cell death), with secondary cascades (apoptosis, glial scarring, neuroinflammation, oxidative stress) developing over subacute-chronic periods [1,4,5]. Despite significant progress in therapeutic strategies, including neurotrophic factor delivery and stem cell-based therapies, the effect of SCI treatment is still not ideal [6–9]. This persistent therapeutic gap underscores the need to identify and validate novel molecular targets capable of synergizing with existing interventions and should be a priority direction for contemporary SCI research.

Huntingtin-associated protein 1 (HAP1), first identified through its interaction with mutant Huntingtin (mHtt), is a neuron-specific scaffold protein existing as two alternatively spliced isoforms: huntingtin-associated protein 1A (HAP1A, 599 amino acids) and huntingtin-associated protein 1B (HAP1B, 629 amino acids), which differ in their C-terminal domains [10,11]. HAP1 knockout (KO) mice display profound postnatal lethality within 5–7 days, primarily attributed to neurodegeneration and suppression of feeding behaviors [12]. Additionally, these mice demonstrate significant deficits in cognitive functions, including impaired spatial learning and reduced recognition memory [12,13].

HAP1 has emerged as a scaffold protein that orchestrates diverse cellular processes, including: signal transduction, vesicular transport, transcriptional regulation, and membrane receptor recycling [14–16]. Mounting evidence demonstrates that HAP1 interacts with multiple trafficking proteins, including dynactin subunit P150Glued (P150^{Glued})

[17], kinesin light chain [18], and kinesin family motor protein 5 [19]. These interactions enable HAP1 to coordinate bidirectional vesicular trafficking, particularly modulating the balance between retrograde and anterograde transport in neurons. Besides, HAP1 interacts with multiple receptors, including epidermal growth factor receptor, γ-amino butyric acid type A receptor, nerve growth factor receptor and tyrosine receptor kinase A [20]. It also regulates neuronal differentiation by promoting neurite outgrowth and synaptic maturation [21–23]. HAP1 is highly expressed in striatal medium spiny neurons (MSNs) and modulates Huntington's disease (HD) progression [24]. HAP1 critically regulates BDNF/TrkB (brain-derived neurotrophic factor/tyrosine receptor kinase B) signaling to modulate neuronal survival and proliferation [15,25]. While these findings establish HAP1's pivotal role in the brain, its spinal cord-specific function remains poorly characterized.

This study demonstrated that HAP1 is predominantly expressed in spinal cord gray matter neurons, indicating neuron-specific regulatory roles. HAP1 heterozygous (HET) female mice exhibited significantly worse morphological and functional recovery post-SCI. Notably, exogenous BDNF administration rescued functional deficits in HET mice, confirming a pivotal role of BDNF in HAP1-mediated repair. RNA-sequencing reveals differentially expressed genes and potential pathways in SCI. These findings establish HAP1 as a master regulator of SCI recovery via BDNF-dependent pathways.

2. Materials and Methods

2.1 Animals

HAP1 genetically modified mice were obtained from the Jackson Laboratory (Strain #007749; Bar Harbor, Maine, USA). HET (heterozygous, $HAP1^{+/-}$) mice were used to generate HET, KO (knockout, $HAP1^{-/-}$) and WT (wild type, $HAP1^{+/+}$) mice. Genotyping was performed through PCR using the following primers: WT 5′-TTTTGGAGGTCTGGTCTCGCTCTG-3′ and 5′-CGTCTTCCATCTTAGTGCGTTCAC-3′, and KO 5′-TTTTGGAGGTCTGGTCTCCGCTCTG-3′ and 5′-CTTCATGTGGATGCTAGGGATCC-3′. Given that KO mice exhibit postnatal lethality within several days [12], HET and WT littermates were used for experiments.

To avoid sex-specific complications (male-predominant urinary retention and mortality post-SCI) [26–28], only female C57BL/6 mice were used in this study.

2.2 Immunofluorescence Staining

Anesthetized mice were transcardially perfused with 0.9% NaCl and 4% paraformaldehyde (Beyotime, Hangzhou, China, P0099-3L) in PBS. T8–T10 spinal cord segments were isolated and post-fixed in 4% paraformaldehyde for 24 h. Tissues were coronally cut into 14-µm sections and blocked in 1% bovine serum albumin (BSA, Beyotime, P0007) with 0.3% Triton X-100 (Beyotime, ST2776-1L) for 1 hour. Sections were immersed in primary antibodies against HAP1 (rabbit, 1:500; Thermo Fisher Scientific, Waltham, MA, USA, cat#: PA5-20377), Nissl (1:1000, Thermo Fisher Scientific, cat#: N21483), Iba1 (goat, 1:400, Novus Biologicals, Centennial, CO, USA, cat#: NB100-1028SS) and GFAP (mouse, 1:2000; Millipore, Burlington, MA, USA, cat#: MAB360) overnight. The following day, sections were dark incubated for 2 hours at room temperature with species-matched Alexa Fluor-conjugated secondary antibodies (1:1000 dilution; Cy3 affinipure goat anti-mouse IgG, cat#: 115-165-003, 1:800, Jackson, West Grove, PA, USA; goat anti-rabbit IgG fluorescein (FITC) cat#: 111-095-003, 1:800, Jackson). Ultimately, sections were stained with DAPI (cat#: h-1200, Vector laboratories, Burlingame, CA, USA) and coverslipped using mounting medium.

2.3 SCI Model

Mice (8 weeks, 23–25 g) were anesthetized and positioned in a stereotaxic frame. The T8–T10 vertebrae were exposed to visualize the dorsal spinal cord. The T9 spinal segment (primary impact zone) was operated on by dropping a 10 g rod (tip diameter: 1.5 mm; impact force: 50 kDyn, 1 Dyn = 10^{-5} N). Mice that received a laminectomy without injury were assigned to the sham group.

2.4 Behavioral Tests

Prior to behavioral testing, all mice underwent a 30 min habituation to acclimatize to the experimental environment. Investigators were blinded to group allocation for behavioral assessment throughout the study.

2.4.1 Basso Mouse Scale (BMS)

Postoperative motor recovery was evaluated using the BMS, a validated scoring system for assessing hindlimb locomotor function [29,30]. Higher score values indicated superior functional recovery (complete paralysis: 0, normal gait: 9).

2.4.2 Forced Swim Test

Mice were forced to swim in a transparent glass tank (45 $\times$ 30 $\times$ 30 cm) containing water at a depth of 20 cm, maintained at 25 $\pm$ 1 °C. Each mouse underwent three 1-minute test sessions separated by 20 min recovery intervals, with all trials recorded by overhead HD video camera. Swim frequency (defined as the number of hindlimb movements per minute) was quantified by blinded observers with group means calculated for statistical comparison.

2.4.3 Inclined Plate Test

Hindlimb muscle strength was assessed in a rectangular glass chamber (45 $\times$ 8 $\times$ 8 cm) with a textured wooden base. The inclination angle was adjusted (typically 30–45°) until each mouse maintained its position for 5 s without slid-

ing down. Three consecutive trials were performed per subject, and time(s) required to descend from maximum elevation to the horizontal plane was recorded, with the mean value used for analysis.

2.4.4 Hot Plate Test

Thermal nociception was assessed using a hot plate test (40 cm high chamber with a metal surface maintained at 55.0 $\pm$ 0.5 °C). Following habituation, mice were individually placed on the heated surface and the latency to first paw withdrawal (defined as clear lifting of hindlimb from the plate) was recorded. Each mouse underwent three trials with 30-min intertrial intervals to prevent thermal sensitization, with the mean withdrawal latency used for statistical analysis.

2.5 Luxol Fast Blue (LFB) Staining

Briefly, tissue sections were stained overnight at 56 °C in LFB (Beyotime, Hangzhou, China, C0631S) solution (0.1% LFB, 0.05% acetic acid in 95% ethanol), followed by sequential washes in 95% ethanol and differentiation in 0.05% lithium carbonate (Li_2CO_3) with 70% ethanol. After thorough rinsing in distilled water, differentiation was arrested by brief immersion in 0.05% Li_2CO_3. Dehydration was completed through a graded ethanol series (70%, 95%, 99%) to ensure optimal myelin visualization.

2.6 RNA Extraction and Quantitative Real-Time Polymerase Chain Reaction (qPCR)

Total RNA was isolated from spinal cord tissue (2 mm around the T9 injury core) using the RNAeasy mini kit (cat#:74104, QIAGEN, Hilden, Germany), followed by cDNA synthesis from 1 µg RNA with the First Strand cDNA Synthesis Kit (cat#: K1622, Thermo Fisher Scientific). For qPCR amplification, we used the Bio-Rad CFX96 system with SYBR Green Master Mix (Applied Biosystems, Shengkang, Bio-Technology Co., Ltd., Suzhou, China) under standardized cycling conditions. The primer sequences for BDNF were F: 5′-CCCACTTTCCCATTCACCGA-3′ and, R: 5′-CCTTCAGCGAGAAGCTCCAT-3′, and for GAPDH, F: 5′-GAGGTAGTTATGGCGTAGTGC-3′ and, R: 5′-CTGGTTTCTGGAGGATGG-3′, with GAPDH used as the endogenous control. Relative quantification was calculated via the $2^{-\Delta\Delta CT}$ method after verifying amplification specificity through melting curve analysis.

2.7 BDNF Enzyme-linked Immunosorbent Assay (ELISA)

Spinal cord tissue samples (2 mm around the T9 injury core) were dissected, homogenized in radio immunoprecipitation assay (RIPA) buffer (Beyotime, Hangzhou, China, P0013E) and centrifuged. Supernatants were collected and diluted 20-fold prior to analysis. BDNF concentration was quantified using a commercial ELISA kit (R&D Systems, cat#: DBNT00027620, Saint Paul, MN, USA) following manufacturer's protocol, with absorbance measured at 450 nm (correction wavelength: 540 nm). Protein normalization was performed using bicinchoninic acid (BCA) assay results, with final BDNF levels expressed as pg/mL.

2.8 Drugs and Administration

BDNF (Sigma-Aldrich) was initially prepared as a 5.0 µg/mL stock solution in 0.9% saline, aliquoted and stored at –80 °C to maintain stability. Immediately prior to intrathecal delivery, stock was diluted in saline to a final therapeutic concentration (20 ng/10 µL). At 7 days post-surgery, injections were performed between the L5–L6 vertebral interspace using a 30-G needle. The injection volume (10 µL) was delivered over 30 s followed by a 60-s needle retention period to ensure complete dispersion and prevent reflux. Normal saline was administered identically as the parallel control.

2.9 RNA Sequence Technology and Bioinformatics Analysis

Spinal cord tissue samples (2 mm around the T9 injury core) were collected from HAP1 HET and WT female mice, with total RNA extracted using the QIAcube Automated System (TIANGEN, Beijing, China). RNA integrity was verified and sequenced at RiboBio Co. (Guangzhou, China). Gene Ontology (GO) enrichment analyzed differentially expressed genes (DEGs, false discovery rate (FDR) <0.05) into biological processes/molecular functions/cellular components; Kyoto Encyclopaedia of Genes and Genomes (KEGG) pathway mapping identified SCI-relevant signaling cascades ($p < 0.01$).

2.10 Statistical Analysis

All quantitative data were analyzed using GraphPad Prism 7.0 (GraphPad Software, La Jolla, CA, USA) with appropriate statistical tests: unpaired *t*-test, one-way ANOVA with Tukey's *post hoc* test, and two-way ANOVA with Bonferroni multiple comparison. All results are presented as mean $\pm$ standard error of the mean (SEM) and statistical significance was defined as $p < 0.05$.

3. Results

3.1 Neuron-specific Localization of HAP1 in Spinal Cord

To characterize the distribution of HAP1, transverse spinal cord sections (T8–T10) were used for immunohistochemistry. HAP1 immunoreactivity exhibited selective enrichment in gray matter regions with minimal expression observed in white matter tracts (Fig. 1A). Double-label staining demonstrated robust colocalization of HAP1 with Nissl bodies, confirming its neuronal-specific expression pattern in spinal cord neurons (Fig. 1A,B). Negligible colocalization was observed between HAP1 and GFAP or Iba1 (Fig. 1C,D), further reinforcing the neuron-specific expression profile of HAP1 in the spinal cord.

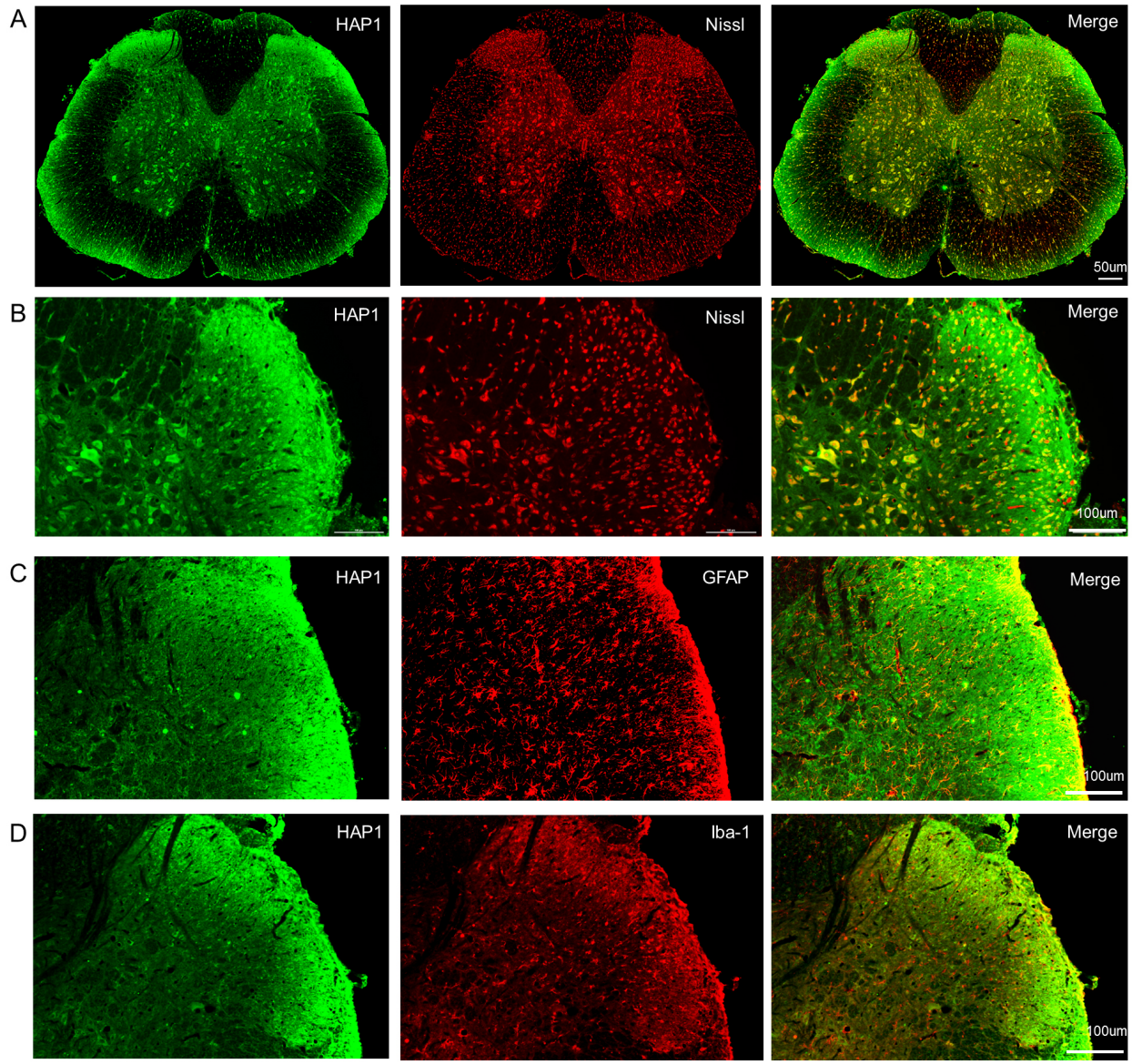

Fig. 1. Fluorescence staining of transverse spinal cord sections (T8–T10) from female mice. (A) HAP1 expression predominantly localized within gray matter regions, exhibiting strong colocalization with Nissl bodies (neuronal marker). Scale bars, 50 µm. (B) Enlarged images demonstrate significant spatial overlap between HAP1 and Nissl bodies in spinal cord neurons. (C,D) Double staining detected negligible colocalization between HAP1 and GFAP (astrocyte marker) or Iba1 (microglia marker). Scale bars, 100 µm. HAP1, huntingtin-associated protein 1; GFAP, glial fibrillary acidic protein.

3.2 Impact of HAP1 Deficiency on Post-SCI Motor Recovery

To elucidate the functional role of HAP1 in SCI recovery, HET mice were utilized due to postnatal lethality in KO mice [12]. HET mice exhibited normal motor function and growth, when compared with WT littermates and post-SCI survival rates showed no genotype-dependent differences. HET mice also displayed significant body weight reduction (Fig. 2A,B), indicating that HAP1 insufficiency may exacerbate injury-induced metabolic dysregulation. Behavioral analyses revealed functional recovery differences between the HET and WT groups. While WT mice demonstrated progressive hindlimb motor improvement, HET mice exhibited persistent motor dysfunction (Fig. 2C). This deficit manifested behaviorally as impaired buoyancy maintenance in forced swim tests and reduced postural stability on inclined plates (Fig. 2D,E).

Notably, negligible differences in nociceptive thresholds were found between the HET and WT groups (Fig. 2F), highlighting HAP1's selective requirement for motor recovery rather than sensory recovery. These results establish HAP1 as a critical regulator of locomotor recovery after spinal cord injury.

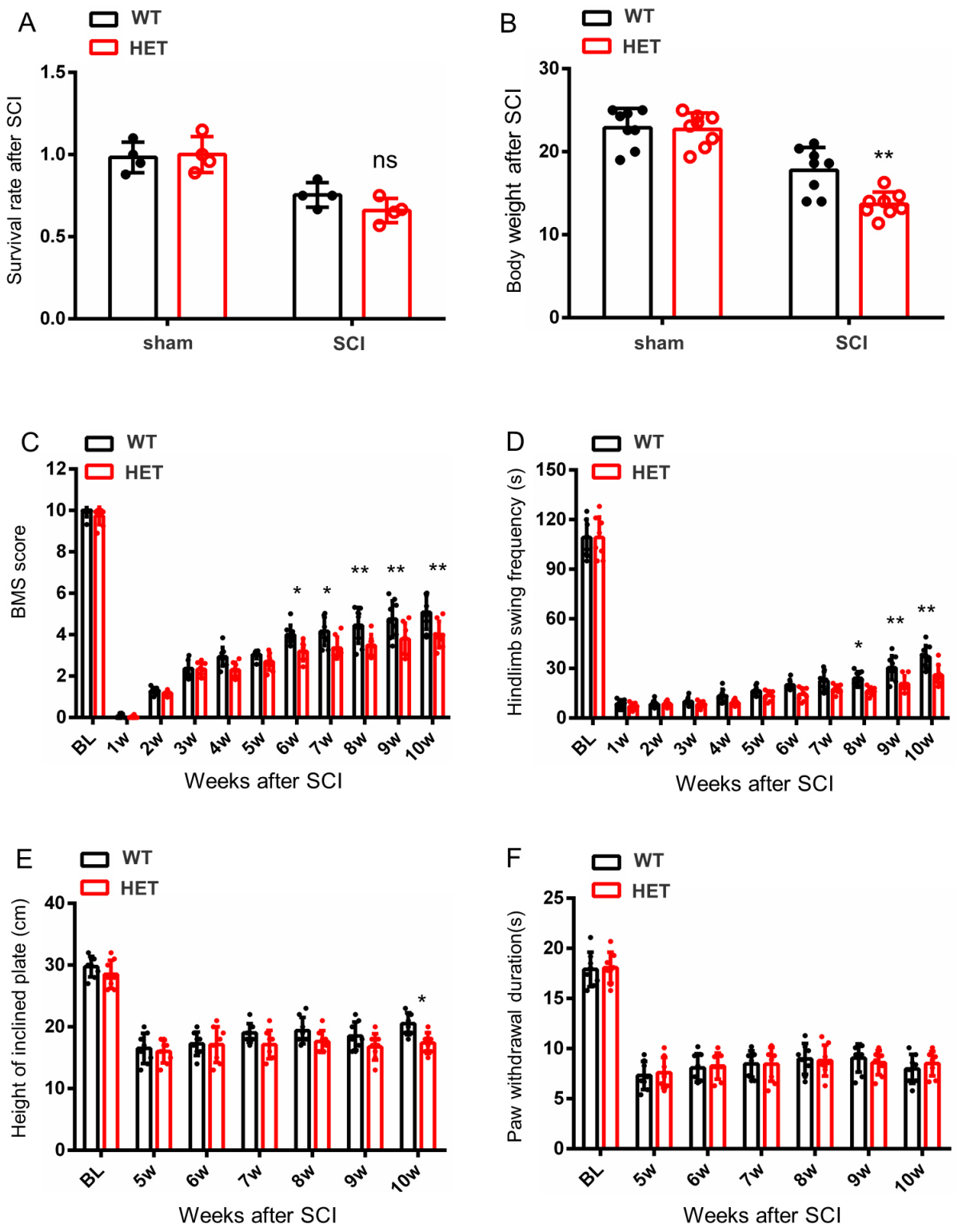

Fig. 2. Behavioral analysis of HET and WT female mice after SCI. (A) Survival rates were comparable between the WT and HET groups both pre- and post-SCI. (B) HET mice exhibited significant weight loss versus WT littermates. (C) BMS revealed enhanced locomotor recovery in WT mice compared with HET mice, with WT mice achieving higher BMS scores. (D) The Swim test showed superior performance in WT mice when compared with HET mice during the chronic phase of SCI. (E,F) No significant intergroup differences between WT and HET mice were found for the inclined plate or hot plate tests. Data are presented as mean ± SEM, one-way or two-way ANOVA, Bonferroni multiple comparisons test; ns, no significance, *$p < 0.05$ and **$p < 0.01$, n = 8/group. HET, heterozygous; WT, wild-type; SCI, spinal cord injury; BMS, Basso mouse scale; SEM, standard error of the mean.

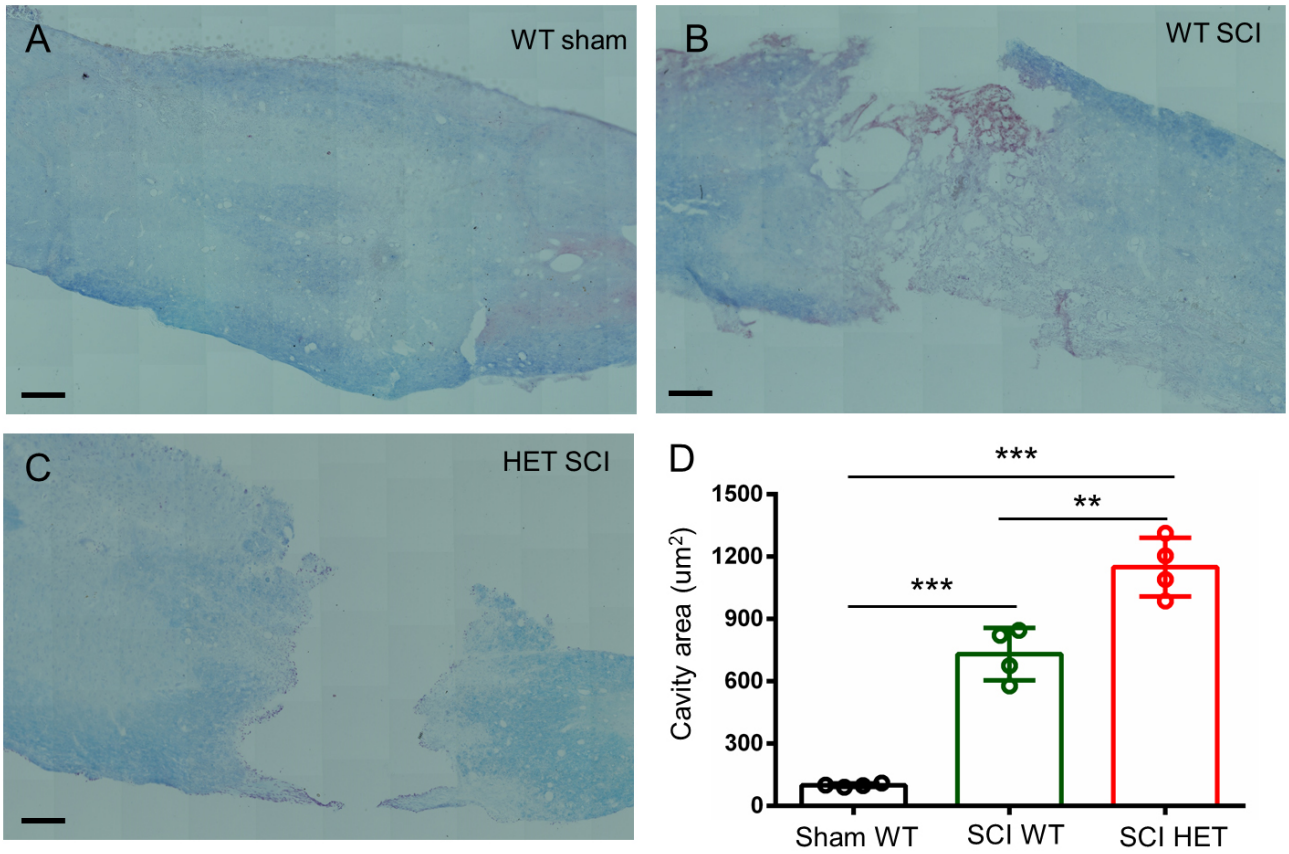

Fig. 3. Histological analysis of T8–T10 spinal cord sections from female mice at 1 month post-SCI using LFB staining. (A) WT sham controls exhibited intact gray/white matter architecture and continuous myelin sheaths. (B,C) Both WT and HET groups showed severe tissue damage, characterized vacuolation, irregular cystic cavities and extensive demyelination. (D) Quantitative analysis demonstrated that HET mice developed larger cystic lesions than WT mice. Scale bars, 100 µm. Mean ± SEM, unpaired *t*-test; $^{**}p < 0.01$, $^{***}p < 0.001$, n = 4/group. LFB, Luxol Fast Blue.

3.3 Impact of HAP1 Deficiency on Post-SCI Morphological Recovery

LFB staining of T8–T10 spinal cord sections at 1month post-SCI was performed to observe structural repair. Sham-operated WT mice exhibited intact architecture with sharp gray/white matter demarcation and robust myelin sheaths (Fig. 3A). Both WT and HET SCI groups exhibited characteristic necrosis, demyelination, and cystic cavitation at the injury epicenter (Fig. 3B,C). Lesion area analysis demonstrated that HET mice developed lesion volumes 33% larger than WT mice (Fig. 3D). HAP1 deficiency weakened structural repair and exacerbated secondary degeneration.

3.4 HAP1 Deficiency Disrupts BDNF Homeostasis During SCI Process

HAP1 serves as a critical neuronal trafficking regulator that facilitates the intracellular transport and activity-dependent secretion of BDNF, thereby establishing HAP1 as a master coordinator of neurotrophic signaling [15,25]. BDNF levels in spinal cord (2 mm around the T9 injury core) were measured using qPCR and ELISA. It was found that WT and HET mice exhibited comparable baseline *BDNF* mRNA expression pre-SCI and both groups showed significant downregulation at 1 month post-injury, with HET mice displaying obviously exacerbated suppression (Fig. 4A). This dysregulation was mirrored at the protein level, where ELISA results demonstrated a greater decrease in mature BDNF in HET than in WT mice (Fig. 4B). These results demonstrate that HAP1 deficiency disrupts BDNF homeostasis during SCI pathogenesis, leading to insufficient neurotrophic support during critical recovery phases.

3.5 BDNF Contributes to Functional Recovery After SCI

To evaluate the therapeutic potential of BDNF, WT and HET mice received daily intrathecal injections of 20 µg BDNF (in 10 µL saline) or vehicle (normal saline) for 3 consecutive days post-SCI (Fig. 5A). Behavioral assessment revealed that intrathecal BDNF administration specifically improved motor function in HET mice after SCI, as evidenced by time-dependent enhancements in BMS scores and swim test performance. Such improvements ultimately

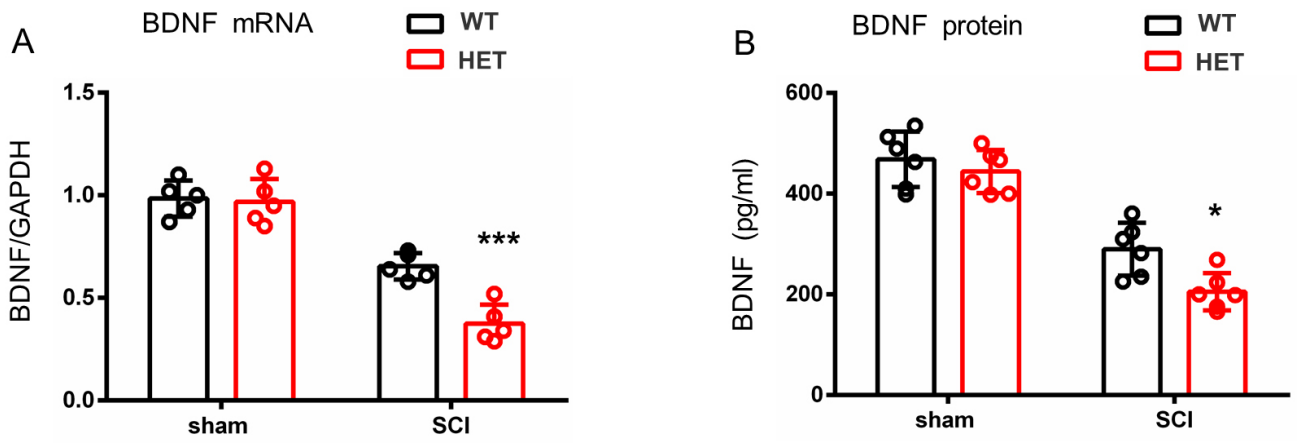

Fig. 4. Quantitative analysis of the injured T9 spinal cord segment at 1 month post-SCI. (A) qPCR demonstrated a greater reduction of *BDNF* mRNA in HET than in WT female mice. (B) ELISA showed protein level suppression, with HET female mice exhibiting lower brain-derived neurotrophic factor (BDNF) than WT counterparts. Mean ± SEM, unpaired *t*-test; **p* < 0.05, ****p* < 0.001, n = 5–6/group. qPCR, quantitative real-time polymerase chain reaction; ELISA, enzyme-linked immunosorbent assay.

surpassed the recovery levels observed in the HET and WT vehicle groups by the chronic phase (Fig. 5B,C), while no significant improvements were detected in sensory or balance in the hot plate and inclined plate tests (Fig. 5D,E). This demonstrates that BDNF's therapeutic effects are selectively targeted to motor circuit plasticity rather than generalized neurological recovery.

3.6 GO Analysis and KEGG Pathway in SCI

To explore the underlying mechanisms associated with HAP1, RNA sequencing (RNA-seq) was performed using RNA extracted from the T8–T10 spinal segments of WT and HET female mice 1 month after SCI. The genetic differences between the WT and HET SCI groups were analyzed from three perspectives: biological process, cellular component, and molecular function. GO analysis revealed that upregulated genes in the WT group were primarily enriched in regulation processes and protein binding (Fig. 6A). DEGs were identified and resulted in 91 upregulated genes and 353 downregulated genes in the WT SCI group when compared with the HET SCI group (Fig. 6B). KEGG pathway enrichment analysis revealed several pathways related to spinal injury, including the nuclear factor kappa-B (NF-κB), tumor necrosis factor (TNF), and cytokine receptor signaling pathways, and the phagosome pathway (Fig. 6C). The results highlighted DEGs between WT and HET mice in the SCI condition, which should be considered as potential targets for further research.

4. Discussion

SCI is a devastating neurological condition triggered by trauma, ischemia, or compression [31]. It initiates a complex pathological cascade characterized by irreversible neuronal death and reactive gliosis with scar formation and progressive cystic cavitation, ultimately leading to chronic sensorimotor deficits and debilitating complications including neuropathic pain, autonomic dysreflexia, and secondary infections [1,6,31]. Current therapeutic paradigms employ two complementary strategies: (1) neuroregenerative approaches (stem cell transplantation, biomaterial scaffolds) targeting neural circuit reconstruction through axonal regrowth facilitation and lesion site repair [32,33] and (2) neuroprotective interventions (anti-inflammatory agents, Rho-kinase inhibitors) aimed at preserving spared neural tissue by mitigating apoptosis and demyelination [34,35]. However, clinical translation remains hampered by the multidimensional nature of SCI pathophysiology, particularly the inhibitory glial microenvironment, deficient axonal guidance cues, and failed synaptic reintegration that collectively underscore the importance of deciphering the spatiotemporal dynamics of molecular and cellular mechanisms governing SCI progression in the development of effective combinatorial therapies.

As the structural and functional core of stigmoid bodies, HAP1 serves as both a defining component and critical biomarker of these neuroprotective organelles [36], with high expression in hypothalamic nuclei and hippocampal and spinal cord dorsal horn, thereby orchestrating multiple neuronal processes, including trafficking, endocytosis, postnatal feeding, and axon growth [37,38]. Central nervous system (CNS) regions with high stigmoid body/HAP1 density demonstrate remarkable resistance to apoptosis, while HAP1 deficient zones consistently develop hallmark pathologies, including polyQ aggregates in Huntington's disease, motor neuron degeneration in spinal muscular atrophy, and progressive Purkinje cell loss in spinocerebellar ataxias [37,39]. While its important roles in the brain are well-documented [40,41], this study explored the possible functions of HAP1 in the spinal cord. Immunofluorescence data demonstrated higher HAP1 intensity in gray

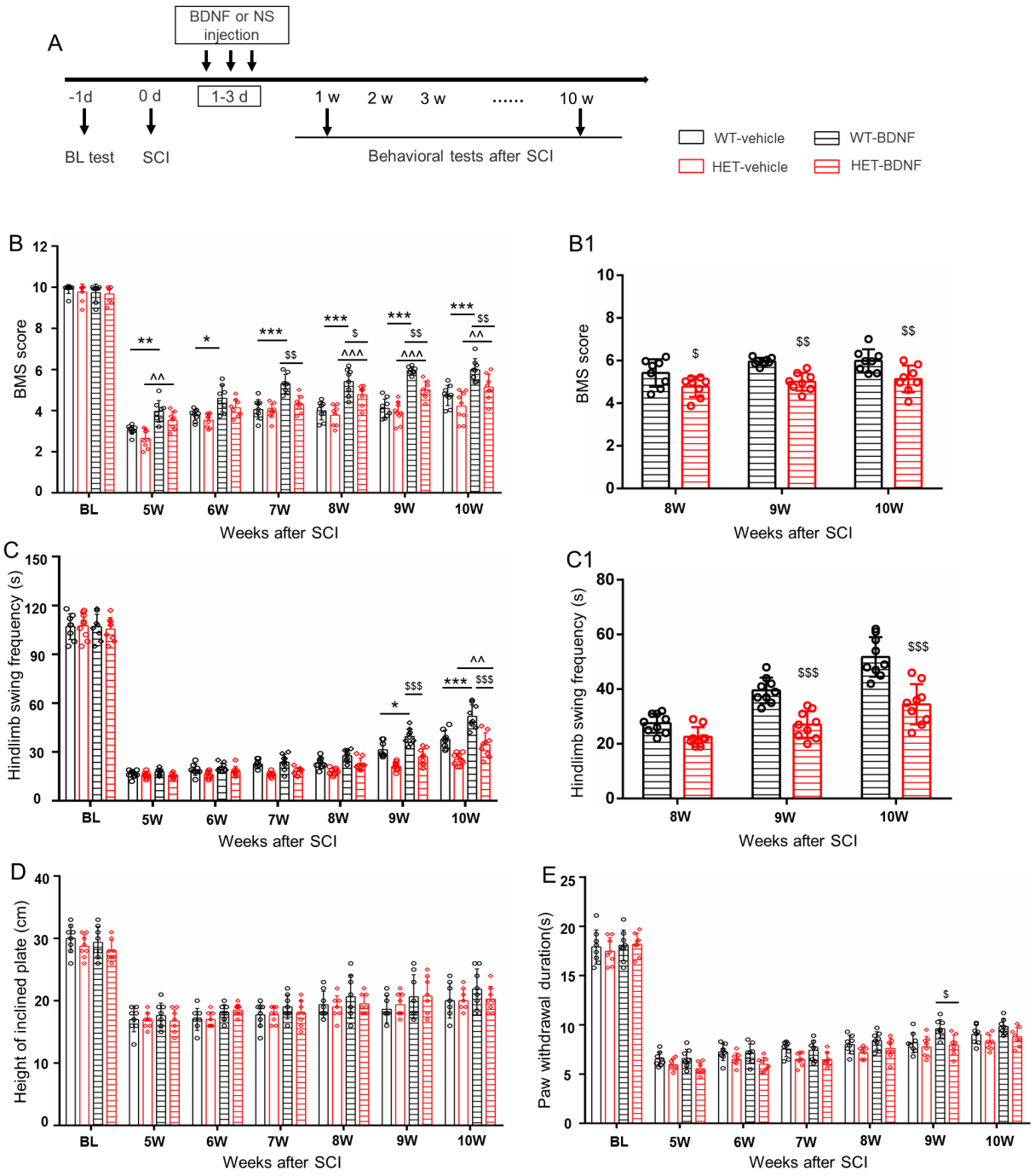

Fig. 5. BDNF enhances motor recovery in HET female mice post-SCI. (A) Schematic illustration of the experimental timeline for BDNF/vehicle administration. (B,C) BDNF administration improved locomotor function in HET female mice after SCI in the BMS and swimming test, when compared with the HET and WT vehicle groups ((B1,C1) panels show function changes in the chronic stages). (D,E) No significant effects were observed in sensory (D) or static balance assessments (E). Mean ± SEM, designated significance markers: * (WT-vehicle *vs.* WT-BDNF), ^ (HET-vehicle *vs.* HET-BDNF), $ (WT-BDNF *vs.* HET-BDNF). Two-way ANOVA with Bonferroni multiple comparisons. */$ $p < 0.05$, ^^/**/$$ $p < 0.01$, ^^^/***/$$$ $p < 0.001$, n = 8–9/group. NS, normal saline.

than in white matter, colocalizing with Nissl$^+$ neurons but complete absence in glial fibrillary acidic protein (GFAP$^+$) astrocytes or Iba1$^+$ microglia, suggesting neuron-exclusive functions in spinal cord that may underlie its observed neuroprotection.

To investigate the functional role of HAP1 in the spinal cord and SCI, longitudinal behavioral assessments in HET and WT female mice were conducted over a 10-week post-injury period. Survival rates and general locomotor activity showed no significant intergroup differences

Fig. 6. Gene expression profiles of WT and HET female mice after SCI. The T8–T10 spinal segments were used for RNA-seq 1 month after surgery. (A) Gene ontology analysis revealed gene expression differences between the WT and HET groups. Upregulated genes were primarily enriched in regulation process and protein binding. (B) Volcano plot of significantly altered genes between the WT and HET groups. Red dot, gene up; green dot, gene down; grey dot, no significant difference. Fold change ≥2, FDR <0.05. (C) KEGG pathway enrichment analysis of differentially expressed genes between the WT and HET groups. The top 30 pathways are shown. Black dot, gene number; purple/green dot, *p* value. FDR, false discovery rate; KEGG, Kyoto Encyclopaedia of Genes and Genomes.

during both pre-injury and acute post-injury phases. Given HAP1's known involvement in insulin secretion regulation, body weight changes were analyzed throughout the 10-week observation period. Notably, HET female mice displayed significantly reduced weight gain when compared with WT littermates, suggesting a potential metabolic influence of HAP1 in the post-SCI recovery process. To assess motor functional recovery, BMS scoring and swim tests were employed. They revealed delayed hindlimb functional restoration in HET female mice relative to WT controls. However, no significant intergroup differences were observed in the inclined plate or hot plate tests. Quantitative histopathological evaluation demonstrated markedly enlarged cystic cavities in HET female mice when compared with WT counterparts. These integrated results indicate that HAP1 deficiency aggravates SCI progression by amplifying both structural damage (cystic cavitation) and functional deficits (hindlimb recovery delay).

In the nervous system, BDNF secretion and transmission play pivotal roles in cell survival, neuronal differentiation, and synaptic plasticity [42–47]. Following synthesis, BDNF undergoes axonal transport and is released in an activity-dependent manner [42,48,49]. Notably, HAP1 exhibits widespread distribution throughout the neural system, including brain, spinal cord, and dorsal root ganglia [37,50,51], where it interacts with multiple membrane proteins regulating vesicular trafficking, particularly those involved in BDNF and pro-BDNF transmission [15,25,42,52]. Building upon this evidence, BDNF expression was quantified via qPCR and ELISA, revealing a marked reduction in both mRNA and protein levels of BDNF in HET mice when compared with WT controls post-SCI. Critically, exogenous BDNF administration significantly enhanced functional recovery, thereby substantiating the hypothesis that HAP1 deficiency impairs behavioral restoration through BDNF downregulation.

Mounting evidence suggests that HAP1 deficiency exacerbates functional impairment after spinal cord injury; however, the precise molecular mechanisms underlying its role in SCI pathophysiology remain elusive. To address this knowledge gap, RNA-seq technology was utilized to comprehensively characterize functional alterations, pathway dysregulation, and transcriptomic changes associated with varying HAP1 expression levels post-SCI. KEGG pathway enrichment analysis revealed significant perturbations across multiple biological domains, including fundamental cellular processes, disease-related pathways, and information transduction systems.

5. Conclusion

This study elucidated the neuroprotective role of HAP1 in SCI pathogenesis and its underlying mechanisms. Abundant HAP1 expression was identified in spinal cord tissues and demonstrated that a genetic deficiency of HAP1 markedly exacerbates both structural damage (cystic cavitation) and functional impairment (hindlimb motor deficits) post-SCI. Mechanistically, these detrimental effects were primarily mediated through significant downregulation of BDNF levels, as evidenced by rescue experiments showing improved behavioral recovery upon exogenous BDNF administration. Transcriptomic profiling revealed gene expression differences in HAP1-deficient conditions, implicating its multifaceted regulatory roles in SCI-related pathological cascades. Collectively, such findings establish HAP1 as a crucial molecule in SCI progression, with the HAP1/BDNF axis representing a promising therapeutic target that merits further investigation.

Availability of Data and Materials

All data generated or analyzed during this study are included in this published article.

Author Contributions

JP and RY designed the research study. XX and YW performed the research. HZ provided help and advice on the ELISA experiments and contributed to the conception of this work. FL analyzed the data. All authors contributed to editorial changes in the manuscript. All authors read and approved the final manuscript. All authors have participated sufficiently in the work and agreed to be accountable for all aspects of the work.

Ethics Approval and Consent to Participate

All procedures were approved by Nantong University's Animal Care Committee (No. S20200323-212) and followed strict ARRIVE guidelines for housing and experimentation.

Acknowledgment

Not applicable.

Funding

This work was supported by the National Natural Science Foundation of China (82001168).

Conflict of Interest

The authors declare no conflict of interest.

References

[1] Wang JL, Luo X, Liu L. Targeting CARD6 attenuates spinal cord injury (SCI) in mice through inhibiting apoptosis, inflammation and oxidative stress associated ROS production. Aging. 2019; 11: 12213–12235. https://doi.org/10.18632/aging.102561.

[2] Cao H, Zhang Y, Chu Z, Zhao B, Wang H, An L. MAP 1B, PACS 2 and AHCYL1 are regulated by miR 34A/B/C and miR 449 in neuroplasticity following traumatic spinal cord injury in rats: Preliminary explorative results from microarray data. Molecular Medicine Reports. 2019; 20: 3011–3018. https://doi.org/10.3892/mmr.2019.10538.

[3] Angeli CA, Rejc E, Ugiliweneza B, Boakye M, Forrest GF, Brockman K, *et al*. Activity-based recovery training with

spinal cord epidural stimulation improves standing performance in cervical spinal cord injury. Journal of Neuroengineering and Rehabilitation. 2025; 22: 101. https://doi.org/10.1186/s12984-025-01636-6.

[4] Marek V, Potey A, Réaux-Le-Goazigo A, Reboussin E, Charbonnier A, Villette T, *et al*. Blue light exposure in vitro causes toxicity to trigeminal neurons and glia through increased superoxide and hydrogen peroxide generation. Free Radical Biology & Medicine. 2019; 131: 27–39. https://doi.org/10.1016/j.freeradbiomed.2018.11.029.

[5] Gu D, Xia Y, Ding Z, Qian J, Gu X, Bai H, *et al*. Inflammation in the Peripheral Nervous System after Injury. Biomedicines. 2024; 12: 1256. https://doi.org/10.3390/biomedicines12061256.

[6] Hurlbert RJ, Hadley MN, Walters BC, Aarabi B, Dhall SS, Gelb DE, *et al*. Pharmacological therapy for acute spinal cord injury. Neurosurgery. 2015; 76: S71–S83. https://doi.org/10.1227/01.neu.0000462080.04196.f7.

[7] Nicola FDC, Marques MR, Odorcyk F, Arcego DM, Petenuzzo L, Aristimunha D, *et al*. Neuroprotector effect of stem cells from human exfoliated deciduous teeth transplanted after traumatic spinal cord injury involves inhibition of early neuronal apoptosis. Brain Research. 2017; 1663: 95–105. https://doi.org/10.1016/j.brainres.2017.03.015.

[8] Li C, Xiang Z, Hou M, Yu H, Peng P, Lv Y, *et al*. miR-NPs-RVG promote spinal cord injury repair: implications from spinal cord-derived microvascular endothelial cells. Journal of Nanobiotechnology. 2024; 22: 590. https://doi.org/10.1186/s12951-024-02797-7.

[9] Ye L, Li W, Tang X, Xu T, Wang G. Emerging Neuroprotective Strategies: Unraveling the Potential of HDAC Inhibitors in Traumatic Brain Injury Management. Current Neuropharmacology. 2024; 22: 2298–2313. https://doi.org/10.2174/1570159X22666240128002056.

[10] Li XJ, Li SH, Sharp AH, Nucifora FC, Jr, Schilling G, Lanahan A, *et al*. A huntingtin-associated protein enriched in brain with implications for pathology. Nature. 1995; 378: 398–402. https://doi.org/10.1038/378398a0.

[11] Li SH, Gutekunst CA, Hersch SM, Li XJ. Association of HAP1 isoforms with a unique cytoplasmic structure. Journal of Neurochemistry. 1998; 71: 2178–2185. https://doi.org/10.1046/j.1471-4159.1998.71052178.x.

[12] Li SH, Yu ZX, Li CL, Nguyen HP, Zhou YX, Deng C, *et al*. Lack of huntingtin-associated protein-1 causes neuronal death resembling hypothalamic degeneration in Huntington's disease. The Journal of Neuroscience. 2003; 23: 6956–6964. https://doi.org/10.1523/JNEUROSCI.23-17-06956.2003.

[13] Sheng G, Chang GQ, Lin JY, Yu ZX, Fang ZH, Rong J, *et al*. Hypothalamic huntingtin-associated protein 1 as a mediator of feeding behavior. Nature Medicine. 2006; 12: 526–533. https://doi.org/10.1038/nm1382.

[14] Czeredys M, Vigont VA, Boeva VA, Mikoshiba K, Kaznacheyeva EV, Kuznicki J. Huntingtin-Associated Protein 1A Regulates Store-Operated Calcium Entry in Medium Spiny Neurons From Transgenic YAC128 Mice, a Model of Huntington's Disease. Frontiers in Cellular Neuroscience. 2018; 12: 381. https://doi.org/10.3389/fncel.2018.00381.

[15] Lim Y, Wu LLY, Chen S, Sun Y, Vijayaraj SL, Yang M, *et al*. HAP1 Is Required for Endocytosis and Signalling of BDNF and Its Receptors in Neurons. Molecular Neurobiology. 2018; 55: 1815–1830. https://doi.org/10.1007/s12035-016-0379-0.

[16] Mackenzie KD, Lim Y, Duffield MD, Chataway T, Zhou XF, Keating DJ. Huntingtin-associated protein-1 (HAP1) regulates endocytosis and interacts with multiple trafficking-related proteins. Cellular Signalling. 2017; 35: 176–187. https://doi.org/10.1016/j.cellsig.2017.02.023.

[17] Engelender S, Sharp AH, Colomer V, Tokito MK, Lanahan A, Worley P, *et al*. Huntingtin-associated protein 1 (HAP1) interacts with the p150Glued subunit of dynactin. Human Molecular Genetics. 1997; 6: 2205–2212. https://doi.org/10.1093/hmg/6.13.2205.

[18] McGuire JR, Rong J, Li SH, Li XJ. Interaction of Huntingtin-associated protein-1 with kinesin light chain: implications in intracellular trafficking in neurons. The Journal of Biological Chemistry. 2006; 281: 3552–3559. https://doi.org/10.1074/jbc.M509806200.

[19] Twelvetrees AE, Yuen EY, Arancibia-Carcamo IL, MacAskill AF, Rostaing P, Lumb MJ, *et al*. Delivery of GABAARs to synapses is mediated by HAP1-KIF5 and disrupted by mutant huntingtin. Neuron. 2010; 65: 53–65. https://doi.org/10.1016/j.neuron.2009.12.007.

[20] Mele M, Aspromonte MC, Duarte CB. Downregulation of $GABA_A$ Receptor Recycling Mediated by HAP1 Contributes to Neuronal Death in In Vitro Brain Ischemia. Molecular Neurobiology. 2017; 54: 45–57. https://doi.org/10.1007/s12035-015-9661-9.

[21] Chen X, Xin N, Pan Y, Zhu L, Yin P, Liu Q, *et al*. Huntingtin-Associated Protein 1 in Mouse Hypothalamus Stabilizes Glucocorticoid Receptor in Stress Response. Frontiers in Cellular Neuroscience. 2020; 14: 125. https://doi.org/10.3389/fncel.2020.00125.

[22] Wu Y, Wang Y, Lu Y, Yan J, Zhao H, Yang R, *et al*. Research advances in huntingtin-associated protein 1 and its application prospects in diseases. Frontiers in Neuroscience. 2024; 18: 1402996. https://doi.org/10.3389/fnins.2024.1402996.

[23] Liu L, Tong H, Sun Y, Chen X, Yang T, Zhou G, *et al*. Huntingtin Interacting Proteins and Pathological Implications. International Journal of Molecular Sciences. 2023; 24: 13060. https://doi.org/10.3390/ijms241713060.

[24] Tang TS, Tu H, Orban PC, Chan EYW, Hayden MR, Bezprozvanny I. HAP1 facilitates effects of mutant huntingtin on inositol 1,4,5-trisphosphate-induced Ca release in primary culture of striatal medium spiny neurons. The European Journal of Neuroscience. 2004; 20: 1779–1787. https://doi.org/10.1111/j.1460-9568.2004.03633.x.

[25] Zamani M, Eslami M, Nezafat N, Hosseini SV, Ghasemi Y. Evaluating the effect of BDNF Val66Met polymorphism on complex formation with HAP1 and Sortilin1 via structural modeling. Computational Biology and Chemistry. 2019; 78: 282–289. https://doi.org/10.1016/j.compbiolchem.2018.12.010.

[26] Wrobel NJ, Shen Q, Kim DH, Adavoody B, Garcia Prada D, Fessler RG, *et al*. Long-term dynamics of the spinal cord injury neuroinflammatory response and sensory dysfunction in female mice. Brain, Behavior, and Immunity. 2025; 129: 143–156. https://doi.org/10.1016/j.bbi.2025.05.024.

[27] St-Pierre MK, González Ibáñez F, Kroner A, Tremblay MÈ. Microglia/macrophages are ultrastructurally altered by their proximity to spinal cord injury in adult female mice. Journal of Neuroinflammation. 2023; 20: 273. https://doi.org/10.1186/s12974-023-02953-0.

[28] Peterson IL, Scholpa NE, Bachtle KJ, Frye JB, Loppi SH, Thompson AD, *et al*. Formoterol alters chemokine expression and ameliorates pain behaviors after moderate spinal cord injury in female mice. The Journal of Pharmacology and Experimental Therapeutics. 2025; 392: 100015. https://doi.org/10.1124/jpet.124.002171.

[29] Bracchi-Ricard V, Lambertsen KL, Ricard J, Nathanson L, Karmally S, Johnstone J, *et al*. Inhibition of astroglial NF-κB enhances oligodendrogenesis following spinal cord injury. Journal of Neuroinflammation. 2013; 10: 92. https://doi.org/10.1186/1742-2094-10-92.

[30] Basso DM, Fisher LC, Anderson AJ, Jakeman LB, McTigue DM, Popovich PG. Basso Mouse Scale for locomotion detects

differences in recovery after spinal cord injury in five common mouse strains. Journal of Neurotrauma. 2006; 23: 635–659. https://doi.org/10.1089/neu.2006.23.635.

[31] Wang XJ, Shu GF, Xu XL, Peng CH, Lu CY, Cheng XY, *et al*. Combinational protective therapy for spinal cord injury medicated by sialic acid-driven and polyethylene glycol based micelles. Biomaterials. 2019; 217: 119326. https://doi.org/10.1016/j.biomaterials.2019.119326.

[32] Uchida S, Hayakawa K, Ogata T, Tanaka S, Kataoka K, Itaka K. Treatment of spinal cord injury by an advanced cell transplantation technology using brain-derived neurotrophic factor-transfected mesenchymal stem cell spheroids. Biomaterials. 2016; 109: 1–11. https://doi.org/10.1016/j.biomaterials.2016.09.007.

[33] Zhang S, Wang XJ, Li WS, Xu XL, Hu JB, Kang XQ, *et al*. Polycaprolactone/polysialic acid hybrid, multifunctional nanofiber scaffolds for treatment of spinal cord injury. Acta Biomaterialia. 2018; 77: 15–27. https://doi.org/10.1016/j.actbio.2018.06.038.

[34] Wang Z, Nong J, Shultz RB, Zhang Z, Kim T, Tom VJ, *et al*. Local delivery of minocycline from metal ion-assisted self-assembled complexes promotes neuroprotection and functional recovery after spinal cord injury. Biomaterials. 2017; 112: 62–71. https://doi.org/10.1016/j.biomaterials.2016.10.002.

[35] Caron I, Papa S, Rossi F, Forloni G, Veglianese P. Nanovector-mediated drug delivery for spinal cord injury treatment. Wiley Interdisciplinary Reviews. Nanomedicine and Nanobiotechnology. 2014; 6: 506–515. https://doi.org/10.1002/wnan.1276.

[36] Islam MN, Miyasato E, Jahan MR, Tarif AMM, Nozaki K, Masumoto KH, *et al*. Mapping of STB/HAP1 Immunoreactivity in the Mouse Brainstem and its Relationships with Choline Acetyltransferase, with Special Emphasis on Cranial Nerve Motor and Preganglionic Autonomic Nuclei. Neuroscience. 2022; 499: 40–63. https://doi.org/10.1016/j.neuroscience.2022.07.016.

[37] Islam MN, Takeshita Y, Yanai A, Imagawa A, Jahan MR, Wroblewski G, *et al*. Immunohistochemical analysis of huntingtin-associated protein 1 in adult rat spinal cord and its regional relationship with androgen receptor. Neuroscience. 2017; 340: 201–217. https://doi.org/10.1016/j.neuroscience.2016.10.053.

[38] Islam MN, Maruyama M, Jahan MR, Afrin M, Meher MM, Nozaki K, *et al*. Neuroanatomical distribution of endogenous huntingtin and its immunohistochemical relationships with STB/HAP1 in the adult mouse brain and spinal cord. Neuroscience Research. 2025; 213: 1–22. https://doi.org/10.1016/j.neures.2025.01.003.

[39] Tarif AMM, Islam MN, Jahan MR, Afrin M, Meher MM, Nozaki K, *et al*. Neurochemical phenotypes of huntingtin-associated protein 1 in reference to secretomotor and vasodilator neurons in the submucosal plexuses of rodent small intestine. Neuroscience Research. 2023; 191: 13–27. https://doi.org/10.1016/j.neures.2022.12.023.

[40] Huang PT, Chen CH, Hsu IU, Salim SA, Kao SH, Cheng CW, *et al*. Huntingtin-associated protein 1 interacts with breakpoint cluster region protein to regulate neuronal differentiation. PLoS ONE. 2015; 10: e0116372. https://doi.org/10.1371/journal.pone.0116372.

[41] Xiang J, Yang S, Xin N, Gaertig MA, Reeves RH, Li S, *et al*. DYRK1A regulates Hap1-Dcaf7/WDR68 binding with implication for delayed growth in Down syndrome. Proceedings of the National Academy of Sciences of the United States of America. 2017; 114: E1224–E1233. https://doi.org/10.1073/pnas.1614893114.

[42] Wu LLY, Fan Y, Li S, Li XJ, Zhou XF. Huntingtin-associated protein-1 interacts with pro-brain-derived neurotrophic factor and mediates its transport and release. The Journal of Biological Chemistry. 2010; 285: 5614–5623. https://doi.org/10.1074/jbc.M109.073197.

[43] Keefe KM, Sheikh IS, Smith GM. Targeting Neurotrophins to Specific Populations of Neurons: NGF, BDNF, and NT-3 and Their Relevance for Treatment of Spinal Cord Injury. International Journal of Molecular Sciences. 2017; 18: 548. https://doi.org/10.3390/ijms18030548.

[44] Leal G, Bramham CR, Duarte CB. BDNF and Hippocampal Synaptic Plasticity. Vitamins and Hormones. 2017; 104: 153–195. https://doi.org/10.1016/bs.vh.2016.10.004.

[45] Wang DP, Yin H, Lin Q, Fang SP, Shen JH, Wu YF, *et al*. Andrographolide enhances hippocampal BDNF signaling and suppresses neuronal apoptosis, astroglial activation, neuroinflammation, and spatial memory deficits in a rat model of chronic cerebral hypoperfusion. Naunyn-Schmiedeberg's Archives of Pharmacology. 2019; 392: 1277–1284. https://doi.org/10.1007/s00210-019-01672-9.

[46] Guan W, Xu DW, Ji CH, Wang CN, Liu Y, Tang WQ, *et al*. Hippocampal miR-206-3p participates in the pathogenesis of depression via regulating the expression of BDNF. Pharmacological Research. 2021; 174: 105932. https://doi.org/10.1016/j.phrs.2021.105932.

[47] Ji CH, Gu JH, Liu Y, Tang WQ, Guan W, Huang J, *et al*. Hippocampal MSK1 regulates the behavioral and biological responses of mice to chronic social defeat stress: Involving of the BDNF-CREB signaling and neurogenesis. Biochemical Pharmacology. 2022; 195: 114836. https://doi.org/10.1016/j.bcp.2021.114836.

[48] Brigadski T, Leßmann V. The physiology of regulated BDNF release. Cell and Tissue Research. 2020; 382: 15–45. https://doi.org/10.1007/s00441-020-03253-2.

[49] Sasi M, Vignoli B, Canossa M, Blum R. Neurobiology of local and intercellular BDNF signaling. Pflugers Archiv: European Journal of Physiology. 2017; 469: 593–610. https://doi.org/10.1007/s00424-017-1964-4.

[50] Islam MN, Maeda N, Miyasato E, Jahan MR, Tarif AMM, Ishino T, *et al*. Expression of huntingtin-associated protein 1 in adult mouse dorsal root ganglia and its neurochemical characterization in reference to sensory neuron subpopulations. IBRO Reports. 2020; 9: 258–269. https://doi.org/10.1016/j.ibror.2020.10.001.

[51] Pan J, Zhao Y, Sang R, Yang R, Bao J, Wu Y, *et al*. Huntington-associated protein 1 inhibition contributes to neuropathic pain by suppressing Cav1.2 activity and attenuating inflammation. Pain. 2023; 164: e286–e302. https://doi.org/10.1097/j.pain.0000000000002837.

[52] Gauthier LR, Charrin BC, Borrell-Pagès M, Dompierre JP, Rangone H, Cordelières FP, *et al*. Huntingtin controls neurotrophic support and survival of neurons by enhancing BDNF vesicular transport along microtubules. Cell. 2004; 118: 127–138. https://doi.org/10.1016/j.cell.2004.06.018.